

Content

Supplementary Figures	2
Figure S1	2
Figure S2	3
Figure S3	4
Figure S4	5
Supplementary Methods	6
Mean-time derivation of k_{cat} and k_{cat}/K_m parameters	6
Kinetic efficiency-accuracy plots for initial section	8
Effective selectivity d_{el}^{nc} and intrinsic selectivity D_I^{nc} of the ribosome	9
Chase of GTPase deficient ternary complex from the ribosome	10
Effect of aminoglycosides on the binding affinity of T_3 or ASL for the ribosome	15
Reduction of a four-state to a three-state scheme for initial codon selection	16
Data analysis	17
Supplementary discussion	18
Kinetics of the chase experiment in near-cognate cases	19
References	22

Supplementary Figures

Figure S1

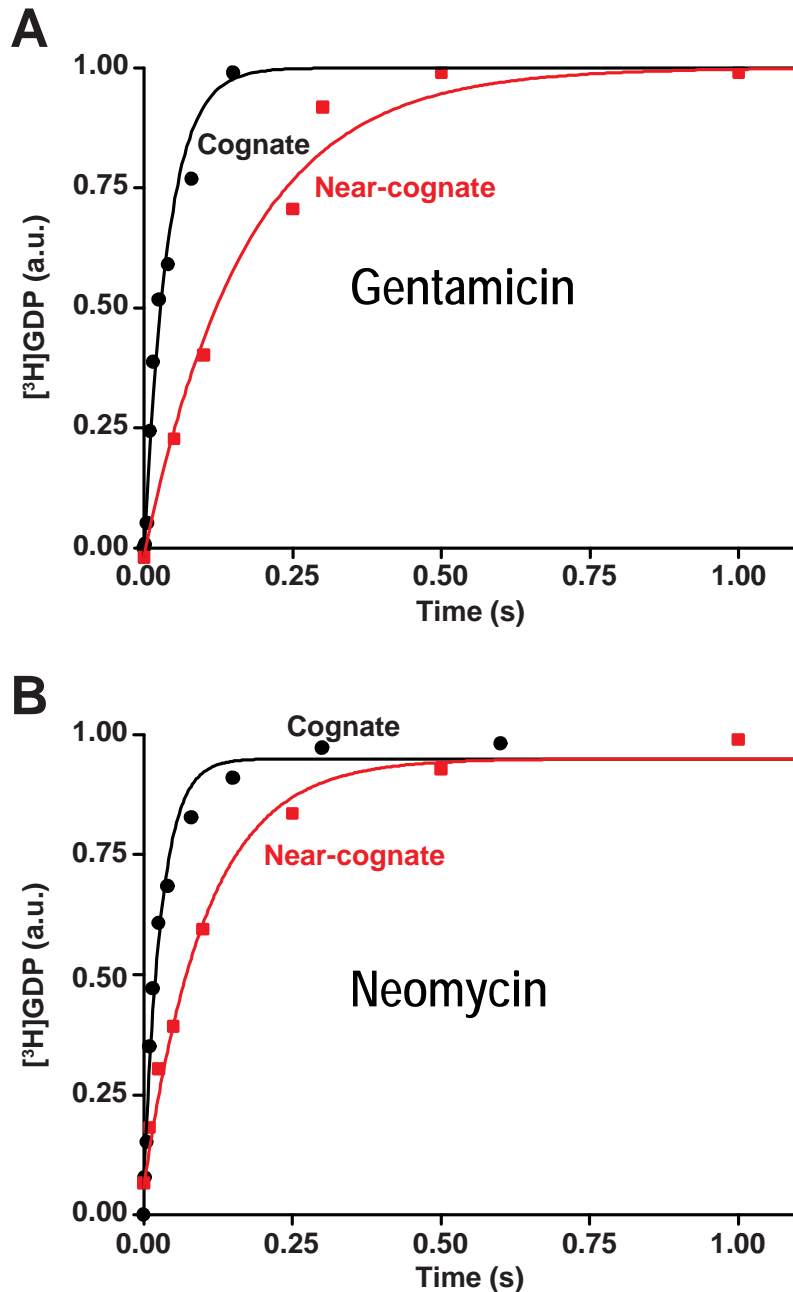


Figure S1. Time course of GTP hydrolysis reaction on $[^3\text{H}]\text{GTP}\cdot\text{EF-Tu}\cdot\text{Phe-tRNA}$ ternary complex reading its cognate codon UUC (●) and near-cognate codon $\underline{\text{C}}\text{UC}$ (■) codon in the presence of drugs. Actual rates, k , of GTP hydrolysis were obtained from single-exponential fits of the curves. Panel A: (Gentamicin) $k=25\text{ s}^{-1}$ for UUC and $k=5.9\text{ s}^{-1}$ for $\underline{\text{C}}\text{UC}$ reading. Panel B: (Neomycin) $k=35\text{ s}^{-1}$ for UUC and $k=9.6\text{ s}^{-1}$ for $\underline{\text{C}}\text{UC}$ reading.

Figure S2

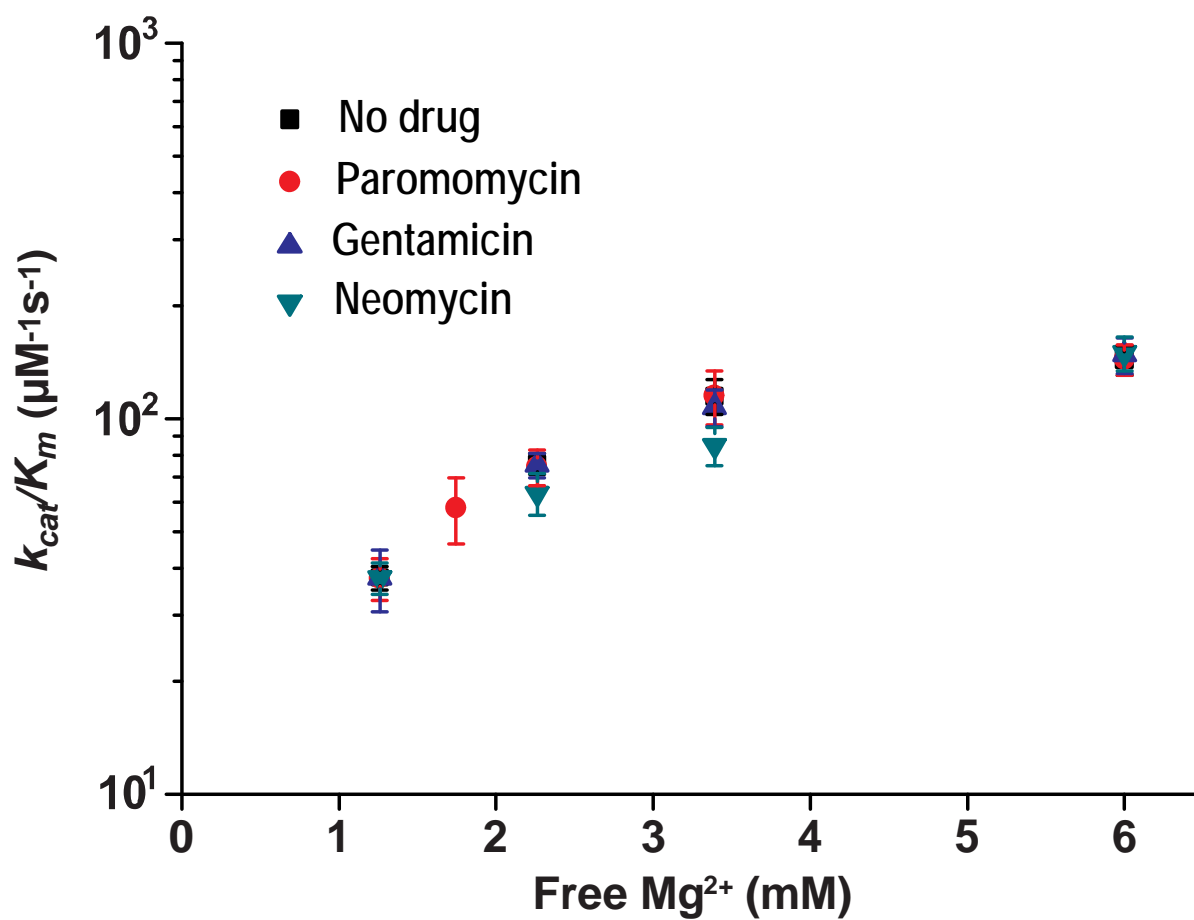


Figure S2. Effect of Mg²⁺ ions and aminoglycosides on the kinetic efficiency k_{cat}/K_m of GTP hydrolysis reaction on [³H]GTP•EF-Tu•Phe-tRNA ternary complex reading its cognate UUC codon in the A site of mRNA programmed ribosome.

Figure S3

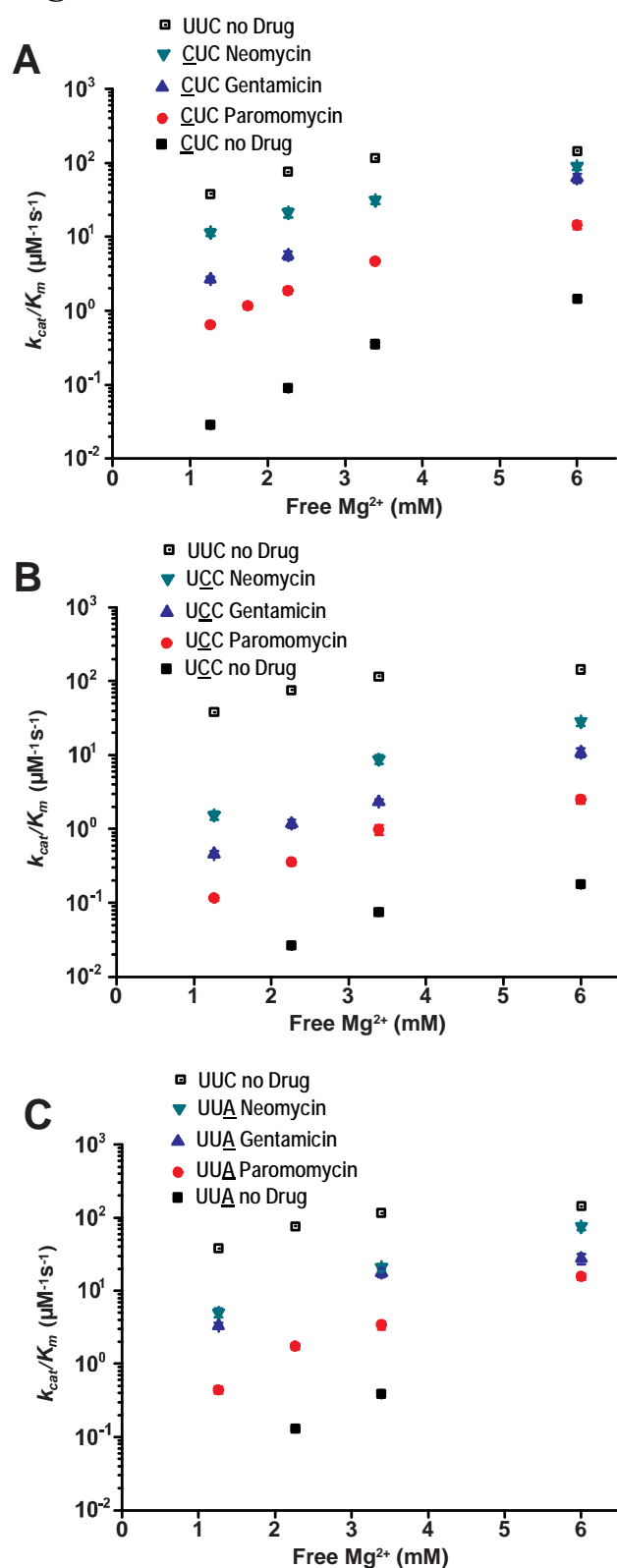


Figure S3. Effect Mg^{2+} ions and aminoglycosides on the kinetic efficiency k_{cat}/K_m of near-cognate codon reading in comparison with that for the reading of the cognate UUC codon in the absence of drug. Panel A: CUC near-cognate codon; Panel B: UCC near-cognate codon; Panel C: UUA near-cognate codon.

Figure S4

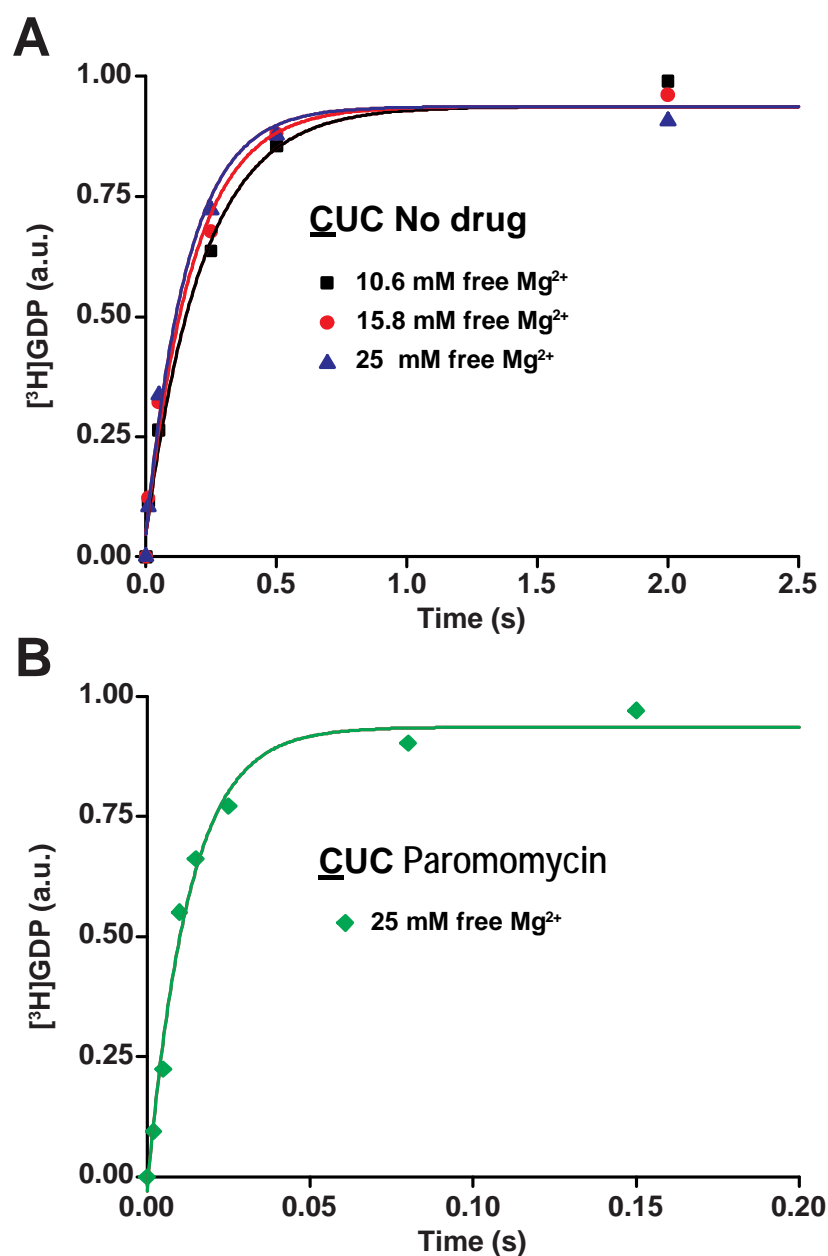
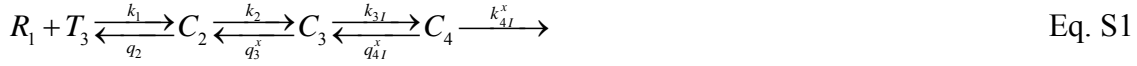


Figure S4. Effect of Mg^{2+} ions and paromomycin on the rate of GTP hydrolysis reaction on $[^3\text{H}]\text{GTP}\cdot\text{EF}\cdot\text{Tu}\cdot\text{Phe}\cdot\text{tRNA}$ ternary complex reading its near-cognate CUC codon in the A site of mRNA programmed ribosome at a near-saturating ribosome concentration. Panel A: $[\text{Mg}^{2+}]$ dependence of the GTP hydrolysis reaction in the absence of drugs. The rate estimated from single exponential fits were: 4.5 s^{-1} at 10.6 mM $[\text{Mg}^{2+}]$; 5.3 s^{-1} at 15.8 mM $[\text{Mg}^{2+}]$ and 6 s^{-1} at 25 mM $[\text{Mg}^{2+}]$. Panel B: The time course of GTP hydrolysis reaction at 25 mM $[\text{Mg}^{2+}]$ in the presence of paromomycin. The rate estimated from a single exponential fit was 79 s^{-1} .

Supplementary Methods

Mean-time derivation of k_{cat} and k_{cat}/K_m parameters

For convenience the four-state scheme in Fig. 5 of the main text is reproduced below:



Michaelis-Menten parameters k_{cat}/K_m and k_{cat} for this scheme are obtained using a mean-time approach (1-3) as follows. The time evolution of probabilities p_1 , p_2 , p_3 and p_4 for ternary complex, T_3 , to be in free state T_3 or in ribosome bound states C_2 , C_3 and C_4 , respectively, is governed by a system of ordinary differential equations:

$$\begin{aligned} \frac{dp_1}{dt} &= -k_1[R_1]p_1 + q_2p_2 \\ \frac{dp_2}{dt} &= k_1[R_1]p_1 - (k_2 + q_2)p_2 + q_3^x p_3 \\ \frac{dp_3}{dt} &= k_2p_2 - (k_{3I} + q_3^x)p_3 + q_{4I}^x p_4 \\ \frac{dp_4}{dt} &= k_{3I}p_3 - (k_{4I}^x + q_{4I}^x)p_4 \end{aligned} \quad \text{Eq. S2}$$

Here $[R_1]$ is the approximately constant concentration of free ribosomes present in excess over ternary complex. Mean times τ_i for T_3 being in states “i” are defined as (1-3):

$$\tau_i = \int_0^{\infty} p_i(t) dt, \quad i=1, 2, 3 \text{ or } 4 \quad \text{Eq. S3}$$

Integrating equation system Eq. S2 from zero to infinite time and taking into account that all ternary complex is free at time zero ($p_1(0)=1$), one obtains the following system of algebraic equations for the mean times τ_i :

$$\begin{aligned} -1 &= -k_1[R_1]\tau_1 + q_2\tau_2 \\ 0 &= k_1[R_1]\tau_1 - (k_2 + q_2)\tau_2 + q_3^x\tau_3 \\ 0 &= k_2\tau_2 - (k_{3I} + q_3^x)\tau_3 + q_{4I}^x\tau_4 \\ 0 &= k_{3I}\tau_3 - (k_{4I}^x + q_{4I}^x)\tau_4 \end{aligned} \quad \text{Eq. S4}$$

Its solution is:

$$\begin{aligned}
\tau_1 &= \frac{1}{k_1[R_1]} \left\{ 1 + \frac{q_2}{k_2} \left(1 + \frac{q_3^x}{k_{3I}} \left(1 + \frac{q_{4I}^x}{k_{4I}^x} \right) \right) \right\} \\
\tau_2 &= \frac{1}{k_2} \left(1 + \frac{q_3^x}{k_{3I}} \left(1 + \frac{q_{4I}^x}{k_{4I}^x} \right) \right) \\
\tau_3 &= \frac{1}{k_{3I}} \left(1 + \frac{q_{4I}^x}{k_{4I}^x} \right) \\
\tau_4 &= \frac{1}{k_{4I}^x}
\end{aligned} \tag{Eq. S5}$$

The mean reaction time starting from free T_3 to GTP hydrolysis is the sum τ of the mean times T_3 spends in states 1, 2, 3 and 4. At low ribosome concentration the mean reaction time is dominated by τ_1 so that in this concentration range τ is inversely proportional to $[R_1]$, and the k_{cat}/K_m parameter is estimated as $1/(\tau [R_1])$:

$$\left(\frac{k_{cat}}{K_m} \right)_I = \frac{1}{\tau [R_1]} = \frac{k_1}{1 + a_2(1 + a_{3I}^x(1 + a_{4I}^x))}, \tag{Eq. S6}$$

where we have introduced “discard” parameters as:

$$\begin{aligned}
a_2 &= q_2 / k_2 \\
a_{3I}^x &= q_3^x / k_{3I} \\
a_{4I}^x &= q_{4I}^x / k_{4I}^x
\end{aligned} \tag{Eq. S7}$$

Discard parameters, a_{yI}^x , determine the probabilities that the ribosomal complexes in Eq. S1 move forward or backward, and a smaller a_{yI}^x -value means a large propensity of forward movement in the scheme. The inverse of a minimal reaction time, obtained in the limit of high ribosome concentration where the contribution of time τ_1 to the total reaction time, τ , is negligible corresponds to the k_{cat}^x parameter of Michaelis-Menten kinetics and is obtained using Eq. S5 as:

$$k_{cat}^x = 1/(\tau_2 + \tau_3 + \tau_4) = 1 / \left[\frac{1}{k_2} (1 + a_{3I}^x(1 + a_{4I}^x)) + \frac{1}{k_{3I}} (1 + a_{4I}^x) + \frac{1}{k_{4I}^x} \right] \tag{Eq. S8}$$

Introduction of the equilibrium constant $K_{23}^x = q_3^x / k_2$ in Eq. S8 leads to :

$$k_{catI}^x = 1 / \left[\frac{1}{k_2} + \frac{1}{k_{4I}^x} + \frac{1}{k_2} \frac{1 + K_{23}^x}{K_{23}^x} a_{3I}^x (1 + a_{4I}^x) \right] \quad \text{Eq. S9}$$

For near-cognate cases the last term in Eq. S9 dominates and we can use Eq. 6 in the main text to recast Eq. S9 as:

$$k_{catI}^{nc} = 1 / \left[\frac{1}{k_2} + \frac{1}{k_{4I}^{nc}} + \frac{1}{k_2} \frac{1 + K_{23}^{nc}}{K_{23}^{nc}} (d_{el}^{nc} - 1) \right] \approx \frac{1}{d_{el}^{nc}} \frac{k_2 K_{23}^{nc}}{1 + K_{23}^{nc}} \quad \text{Eq. S10}$$

It follows, therefore, that the k_{catI}^{nc} increase by aminoglycosides is expected to be inversely proportional to the decrease in the effective selectivity d_{el}^{nc} induced by their presence.

Kinetic efficiency-accuracy plots for initial section

The accuracy, A, of initial codon selection is defined by the ratio between cognate and near-cognate k_{cat}/K_m -values (4):

$$A = \frac{(k_{cat} / K_m)^c}{(k_{cat} / K_m)^{nc}} = \frac{1 + a_2(1 + a_{3I}^{nc}(1 + a_{4I}^{nc}))}{1 + a_2(1 + a_{3I}^c(1 + a_{4I}^c))} \quad \text{Eq.S11}$$

Introducing effective selectivity parameter d_{el}^{nc} :

$$d_{el}^{nc} = \frac{1 + a_{3I}^{nc}(1 + a_{4I}^{nc})}{1 + a_{3I}^c(1 + a_{4I}^c)} \quad \text{Eq. S12}$$

and using Eq. S6 for cognate $(k_{cat} / K_m)^c$, Eq. S11 can be re-written as

$$\begin{aligned} A_I^{nc} &= \frac{(k_{cat} / K_m)_I^c}{k_1} \left\{ 1 + d_{el}^{nc} a_2 (1 + a_{3I}^c (1 + a_{4I}^c)) \right\} = \\ &= \frac{(k_{cat} / K_m)_I^c}{k_1} \left\{ 1 - d_{el}^{nc} + d_{el}^{nc} \frac{k_1}{(k_{cat} / K_m)_I^c} \right\} = \frac{(k_{cat} / K_m)_I^c}{k_1} (1 - d_{el}^{nc}) + d_{el}^{nc} \end{aligned} \quad \text{Eq. S13}$$

Solving this equation for $(k_{cat} / K_m)_I^c$ one obtains Eq. 1 of the main text:

$$\left(\frac{k_{cat}}{K_M} \right)_I^c = k_1 \frac{d_{el}^{nc} - A_I^{nc}}{d_{el}^{nc} - 1} \quad \text{Eq. S14}$$

Effective selectivity d_{el}^{nc} and intrinsic selectivity D_I^{nc} of the ribosome

Taking into account that for cognate discard parameters $a_{3I}^c \ll 1$, $a_{4I}^c \ll 1$ and that $a_{4I}^{nc} \gg 1$ in near-cognate cases (see the explanation in the main text) effective selectivity d_{el}^{nc} defined by

Eq. S12 is approximated as:

$$d_{el}^{nc} \approx 1 + a_{3I}^{nc} a_{4I}^{nc} \quad \text{Eq. S15}$$

Using the definition of discard parameters in Eq. S7 this relation can be presented as:

$$d_{el}^{nc} - 1 \approx a_{3I}^{nc} a_{4I}^{nc} = \frac{q_3^{nc} q_{4I}^{nc}}{k_{3I} k_{4I}^{nc}} = K_{34I}^{nc} \frac{q_3^{nc}}{k_{4I}^{nc}} = K_{34I}^{nc} \frac{q_3^{nc} k_2}{k_{4I}^{nc} k_2} = K_{23}^{nc} K_{34I}^{nc} \frac{k_2}{k_{4I}^{nc}} \quad \text{Eq. S16}$$

Here we used the definition of equilibrium constants K_{23}^x and K_{34I}^x connecting state (C₂, C₃) and (C₃, C₄), respectively:

$$\begin{aligned} K_{23}^x &= q_3^x / k_2 \\ K_{34I}^x &= q_{4I}^x / k_{3I} \end{aligned} \quad \text{Eq. S17}$$

Taking into account that $d_{el}^{nc} \approx d_{el}^{nc} - 1$ for large d_{el}^{nc} values, Eq. S16 explains Eq. 12 of the main text. From Eq. S16 one obtains:

$$\frac{d_{e0}^{nc} - 1}{d_{el}^{nc} - 1} \approx \frac{a_{30}^{nc} a_{40}^{nc}}{a_{3I}^{nc} a_{4I}^{nc}} = \frac{K_{23}^{nc} K_{340}^{nc} k_{4I}^{nc}}{K_{23}^{nc} K_{34I}^{nc} k_{40}^{nc}} = \frac{K_{340}^{nc} k_{4I}^{nc}}{K_{34I}^{nc} k_{40}^{nc}} \quad \text{Eq. S18}$$

Again, using that $d_{el}^{nc} \gg 1$ and $d_{e0}^{nc} \gg 1$, Eq. S18 explains Eq.13 of the main text.

We now express the intrinsic selectivity D_I^{nc} given by Eq. 7 of the main text through the rates and equilibrium constants (Eq. S17) of the scheme in Eq. S1 as:

$$D_I^{nc} = \frac{a_{3I}^{nc} a_{4I}^{nc}}{a_{3I}^c a_{4I}^c} = \left(\frac{q_3^{nc} q_{4I}^{nc}}{k_{3I} k_{4I}^{nc}} \right) / \left(\frac{q_3^c q_{4I}^c}{k_{3I} k_{4I}^c} \right) = \frac{K_{23}^{nc} K_{34I}^{nc} k_{4I}^c}{K_{23}^c K_{34I}^c k_{4I}^{nc}} \quad \text{Eq. S19}$$

Further, using also that the equilibrium constant $K_{12} = q_2 / k_1$ for T_3 and R_1 to form complex C₂ is the same in cognate and near-cognate cases one obtains:

$$D_I^{nc} = \frac{K_{12} K_{23}^{nc} K_{34I}^{nc} k_{4I}^c}{K_{12} K_{23}^c K_{34I}^c k_{4I}^{nc}} = \exp \left[(\Delta G_{1,\#}^{nc} - \Delta G_{1,\#}^c) / RT \right] \quad \text{Eq. S20}$$

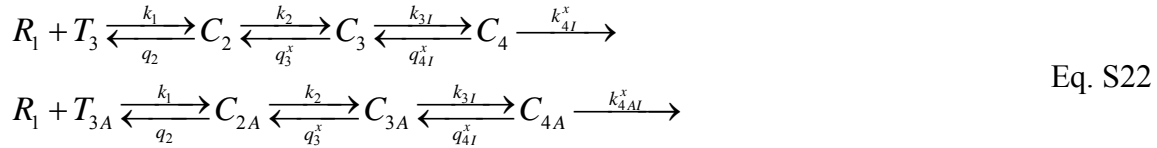
In the case $k_{4I}^{nc} \approx k_{4I}^c$ Eq. S19 simplifies to:

$$D_I^{nc} = \frac{K_{23}^{nc} K_{34I}^{nc}}{K_{23}^c K_{34I}^c} = \exp\left[\frac{(\Delta G_{2,4}^{nc} - \Delta G_{2,4}^c)}{RT}\right] \quad \text{Eq. S21}$$

Assuming that the standard free energy of state C_2 is the same for cognate and near-cognate T_3 s the difference $\Delta G_{2,4}^{nc} - \Delta G_{2,4}^c$ corresponds to the difference in standard free energy for near-cognate and cognate codon-anticodon helices in state C_4 .

Chase of GTPase deficient ternary complex from the ribosome

We now estimate the mean time of GTPase reaction on a native ternary complex T_3 chasing a GTPase deficient ternary complex T_{3A} assembled with GTPase deficient EF-Tu mutant in which His84 is replaced with Ala (5). Assuming that the native and mutant ternary complexes are identical, except that the mutant T_{3A} hydrolyzes GTP extremely slow (5), we can describe GTPase reaction by the following scheme:



Here, k_{4AI}^x is the rate constant of GTP hydrolysis on the EF-Tu_{H84A} mutant in T_{3A} . The probabilities p_2 , p_3 and p_4 are the probabilities of the ribosome to be in states C_2 , C_3 and C_4 with bound native T_3 , respectively. The probabilities p_{2A} , p_{3A} and p_{4A} are the probabilities of the ribosome to be in states C_{2A} , C_{3A} and C_{4A} with bound mutant T_{3A} , respectively. The probabilities p_1 is the probability of the ribosome to be free.

The system of differential equations that describes the time evolution of these probabilities is:

$$\begin{aligned}
\frac{dp_1}{dt} &= -(k_1 [T_3] + k_1 [T_{3A}])p_1 + q_2 p_2 \\
\frac{dp_2}{dt} &= k_1 [T_3] p_1 - (k_2 + q_2)p_2 + q_3^x p_3 \\
\frac{dp_3}{dt} &= k_2 p_2 - (k_{3I} + q_3^x)p_3 + q_{4I}^x p_4 \\
\frac{dp_4}{dt} &= k_{3I} p_3 - (k_{4I}^x + q_{4I}^x)p_4 \\
\frac{dp_{2A}}{dt} &= k_1 [T_{3A}] p_1 - (k_2 + q_2)p_{2A} + q_3^x p_{3A} \\
\frac{dp_{3A}}{dt} &= k_2 p_{2A} - (k_{3I} + q_3^x)p_{3A} + q_{4I}^x p_{4A} \\
\frac{dp_{4A}}{dt} &= k_{3I} p_{3A} - (k_{4AI}^x + q_{4I}^x)p_{4A}
\end{aligned} \tag{Eq. S23}$$

The algebraic equation system for the corresponding mean times is obtained by integrating equation system Eq. S23 from zero to infinite time given that all ribosomes are originally in state C_{4A} (i.e. $p_{4A}(0)=1$) :

$$\begin{aligned}
0 &= -(k_1 [T_3] + k_1 [T_{3A}])\tau_1 + q_2 \tau_2 \\
0 &= k_1 [T_3] \tau_1 - (k_2 + q_2)\tau_2 + q_3^x \tau_3 \\
0 &= k_2 \tau_2 - (k_{3I} + q_3^x)\tau_3 + q_{4I}^x \tau_4 \\
0 &= k_{3I} \tau_3 - (k_{4I}^x + q_{4I}^x)\tau_4 \\
0 &= k_1 [T_{3A}] \tau_1 - (k_2 + q_2)\tau_{2A} + q_3^x \tau_{3A} \\
0 &= k_2 \tau_{2A} - (k_{3I} + q_3^x)\tau_{3A} + q_{4I}^x \tau_{4A} \\
-1 &= k_{3I} \tau_{3A} - (k_{4AI}^x + q_{4I}^x)\tau_{4A}
\end{aligned} \tag{Eq. S24}$$

Solving this algebraic system and taking into account the definitions of discard parameters in Eq. S7, one obtains mean times of the states in the upper branch of the scheme in Eq. S22 as:

$$\begin{aligned}
\tau_1 &= \frac{1}{k_1 [T_3]} \left\{ 1 + a_2 (1 + a_{3I}^x (1 + a_{4I}^x)) \right\} k_{4I}^x \tau_4 \\
\tau_2 &= \frac{1}{k_2} (1 + a_{3I}^x (1 + a_{4I}^x)) k_{4I}^x \tau_4 \\
\tau_3 &= \frac{1}{k_{3I}} (1 + a_{4I}^x) k_{4I}^x \tau_4
\end{aligned} \tag{Eq.S25}$$

Summing up all the equations of equation system S24 one also obtains $k_{4I}^x \tau_4 + k_{4IA}^x \tau_{4A} = 1$. It follows that the product $k_{4I}^x \tau_4$ in Eq. S25 has the meaning of the fraction of GTP hydrolyzed through the upper branch of the scheme in Eq. S22. For the low branch one obtains:

$$\begin{aligned}\tau_{2A} &= \frac{1}{q_2} k_{4I}^x \tau_4 + \frac{k_1 [T_{3A}]}{q_2} \tau_1 \\ \tau_{3A} &= \frac{1}{q_3} \left(1 + \frac{k_2}{q_2}\right) k_{4I}^x \tau_4 + \frac{k_2 k_1 [T_{3A}]}{q_3 q_2} \tau_1 \\ \tau_{4A} &= \left\{ \frac{1}{q_{4I}^x} + \frac{1}{q_3} \frac{k_{3I}}{q_{4I}^x} \left(1 + \frac{k_2}{q_2}\right) \right\} k_{4I}^x \tau_4 + \frac{k_{3I} k_2 k_1 [T_{3A}]}{q_{4I}^x q_3 q_2} \tau_1\end{aligned}\tag{Eq. S26}$$

The sum, τ_{ch} , of the mean times in the low branch of Eq. S22 dominates the total mean time of GTP hydrolysis:

$$\begin{aligned}\tau_{ch} &= \tau_{2A} + \tau_{3A} + \tau_{4A} = \frac{k_1 [T_{3A}]}{q_2} k_2 \tau_1 \left(\frac{1}{k_2} + \left(1 + \frac{k_{3I}}{q_{4I}^x}\right) \frac{1}{q_3} \right) + \\ &+ \left\{ \frac{1}{q_2} + \frac{1}{q_{4I}^x} + \frac{1}{q_3} \left(1 + \frac{k_{3I}}{q_{4I}^x}\right) \left(1 + \frac{k_2}{q_2}\right) \right\} k_{4I}^x \tau_4\end{aligned}\tag{Eq. S27}$$

Taking into account that in the cognate case the equilibrium is strongly shifted to state C4 relative state C3, and hence, $K_{34I}^c = q_{4I}^c / k_{3I} \ll 1$, and using definitions of discard parameters in Eq.S7 one simplifies Eq. S27 to:

$$\tau_{ch} \approx k_1 [T_{3A}] \frac{\tau_1}{a_2} \left(\frac{1}{k_2} + \frac{1}{q_{4I}^c a_{3I}^c} \right) + \left\{ \frac{1}{q_2} + \frac{1 + a_2 (1 + a_{3I}^c)}{q_{4I}^c a_2 a_{3I}^c} \right\} k_{4I}^c \tau_4\tag{Eq. S28}$$

In the cognate case $a_{3I}^c \ll 1$ and $a_{4I}^c \ll 1$ both in the presence and absence of aminoglycosides. Using this and the explicit expression for τ_1 from Eq. S25 one obtains:

$$\tau_{ch} \approx \left[\left\{ 1 + \frac{[T_{3A}]}{[T_3]} \right\} \frac{1 + a_2}{a_2} \cdot \frac{1}{q_{4I}^c a_{3I}^c} + \frac{[T_{3A}]}{[T_3]} \frac{1 + a_2}{a_2} \left(\frac{1}{k_2} + \frac{1}{q_3} \right) + \frac{1}{q_2} \right] k_{4I}^c \tau_4\tag{Eq. S29}$$

The last term in the expression in square brackets, $1/q_2$ is very small at low Mg^{2++} concentration, the rate constant k_2 should be faster than the k_{cat} of cognate GTP hydrolysis and, hence, $1/k_2$ is also very small. Neglecting these two terms in Eq. S29 one obtains:

$$\tau_{ch} \approx \frac{1+a_2}{a_2} \left(\frac{1}{q_3^c} \right) \left[\left\{ 1 + \frac{[T_{3A}]}{[T_3]} \right\} \cdot \frac{1}{K_{34I}^c} + \frac{[T_{3A}]}{[T_3]} \right] (1 - k_{4AI}^c \tau_{4A}) \quad \text{Eq. S30}$$

Here, $k_{4AI}^c \tau_{4A}$ is the fraction of GTP hydrolysis due to a very slow GTPase activity of the mutant EF-Tu in T_{3A} . We note that $k_{4AI}^c \tau_{4A}$ is always smaller than one since $k_{4I}^c \tau_4 + k_{4IA}^c \tau_{4A} = 1$.

Taking into account that in cognate cases $K_{34I}^c \ll 1$, the expression above shows that the first term in the expression in square brackets in Eq. S29 and Eq. S30 dominates τ_{ch} . Under standard conditions of chase experiment $[T_3] \gg [T_{3A}]$ and assuming that $k_{4AI}^c \tau_{4A}$ can be neglected, one obtains a genuine mean dissociation time of GTPase deficient ternary complex as (see Eq. S30):

$$\tau_{diss,I} = \frac{1+a_2}{a_2} \cdot \frac{1}{K_{4I}^c q_3^c} = \frac{1+a_2}{a_2} \cdot \frac{1}{q_{4I}^c a_{3I}^c} = \frac{1+a_2}{a_2} \cdot \frac{1}{k_{4I}^c a_{3I}^c a_{4I}^c} \quad \text{Eq. S31}$$

Eq. S31 explains Eq. 10 of the main text. Moreover, using Eq. S31 one obtains for the ratio

$$\tau_{diss,I}^c / \tau_{diss,0}^c :$$

$$\frac{\tau_{diss,I}^c}{\tau_{diss,0}^c} = \frac{a_{30}^c a_{40}^c k_{4I}^c}{a_{3I}^c a_{4I}^c k_{40}^c} = \frac{a_{30}^c q_{40}^c}{a_{3I}^c q_{4I}^c} = \frac{q_3^c k_{3I}^c q_{40}^c}{q_3^c k_{30}^c q_{4I}^c} = \frac{K_{340}^c}{K_{34I}^c} \quad \text{Eq. S32}$$

Eq. S30 shows that the increase in mean dissociation time of GTPase deficient T_3 corresponds to the decrease in equilibrium constant K_{340}^c by an aminoglycoside.

It is easy to show that τ_{4A} given by Eq.S26 coincides with τ_{ch} given by Eq. S30, *i.e.* $\tau_{ch} \approx \tau_{4A}$ and the chase time is dominated by τ_{4A} . Further, setting $\tau_{4A} = \tau_{ch}$ in Eq. S30, the genuine dissociation time $\tau_{diss,I}$ can now be obtained from the chase time τ_{ch} determined at

arbitrary T_3 and T_{3A} concentration and under conditions when the fraction , $k_{4AI}^c \tau_{4A}$, of GTP hydrolyzed by the mutant EF-Tu in T_{3A} cannot be neglected:

$$\tau_{diss,I} \approx \tau_{ch} \cdot \frac{[T_3]}{[T_{3A}] + [T_3]} \cdot \frac{1}{1 - k_{4AI}^c \tau_{ch}} \quad \text{Eq. S33}$$

Here, the last term in Eq. S33 is estimated using the experimentally measured rate $k_{4AI}^c \approx 0.0024 \text{ s}^{-1}$ of dipeptide formation with T_{3A} in the absence of chase. We note that this rate, measured here at 37°C is about eight fold faster than the GTP hydrolysis rate of 0.0003 s^{-1} at 20°C measured for EF-Tu_{H84A} previously (5). The chase time τ_{ch} dominates GTP hydrolysis time, τ_{GTP} , and also the time, τ_{dip} , of dipeptide formation measured in our chase experiments so that $\tau_{ch} \approx \tau_{dip}$. Eq. S33 explains, therefore, both the first correction factor $\{1 + [T_{3A}]/[T_3]\}$ and also the second correction factor $(1 - k_{4AI}^c \tau_{ch})$ we used to obtain $\tau_{diss,I}$ from experimentally measured τ_{dip} .

Combining the approximate equality $\tau_{disI}^c / \tau_{dis0}^c \approx d_{e0}^{nc} / d_{eI}^{nc}$ with Eq. S32 and Eq. S18 one obtains:

$$\frac{a_{30}^c a_{40}^c k_{4I}^c}{a_{3I}^c a_{4I}^c k_{40}^c} = \frac{\tau_{disI}^c}{\tau_{dis0}^c} \approx \frac{d_{e0}^{nc}}{d_{eI}^{nc}} \approx \frac{a_{30}^{nc} a_{40}^{nc}}{a_{3I}^{nc} a_{4I}^{nc}} \quad \text{Eq. S34}$$

It can be recast as:

$$\frac{a_{3I}^{nc} a_{4I}^{nc}}{a_{30}^{nc} a_{40}^{nc}} \approx \frac{a_{30}^{nc} a_{40}^{nc}}{a_{3I}^{nc} a_{4I}^{nc}} \cdot \frac{k_{40}^c}{k_{4I}^c} \quad \text{Eq. S35}$$

Taking then into account the definition of intrinsic selectivity (see Eq. S19) one obtains:

$$D_I^{nc} \approx D_0^{nc} \cdot \frac{k_{40}^c}{k_{4I}^c} \quad \text{Eq. S36}$$

This corresponds to Eq. 11 of the main text.

To obtain Eq. 13 of the main text we again combine the approximate equality

$\tau_{disI}^c / \tau_{dis0}^c \approx d_{e0}^{nc} / d_{el}^{nc}$ with Eq. S32 and Eq. S18 in which discard parameters are expressed

through equilibrium constants of the scheme in Eq. S1. One obtains:

$$\frac{K_{340}^c}{K_{34I}^c} = \frac{\tau_{disI}^c}{\tau_{dis0}^c} \approx \frac{d_{e0}^{nc}}{d_{el}^{nc}} \approx \frac{K_{340}^{nc}}{K_{34I}^{nc}} \cdot \frac{k_{4I}^{nc}}{k_{40}^{nc}} \quad \text{Eq. S37}$$

It corresponds to Eq. 13 on the main text.

Effect of aminoglycosides on the binding affinity of T_3 or ASL for the ribosome

The overall affinity of a ternary complex T_3 , assembled with GTPase deficient EF-Tu, to the ribosome depends in a simple manner on its binding affinities to the different ribosomal states in the scheme in Fig. 5 of the main text (see also Eq. S1 of SI). First we note that:

$$\begin{aligned} [C_2] &= [R_1][T_3^x] / K_{12} \\ [C_3] &= [C_2] / K_{23}^x \\ [C_4] &= [C_3] / K_{34I}^x = [C_2] / (K_{23}^x K_{34I}^x) \end{aligned} \quad \text{Eq. S38}$$

The fraction of unbound ribosomes is then obtained as:

$$\frac{[R_1]}{[R_{tot}]} = \left\{ 1 + [T_3^x] \frac{1}{K_{12}} \left(1 + \frac{1}{K_{23}^x} \left(1 + \frac{1}{K_{34I}^x} \right) \right) \right\}^{-1} \quad \text{Eq. S39}$$

The effective equilibrium dissociation constant K_{dl}^x between free and T_3 -bound ribosomes is

then given by:

$$K_{dl}^x = K_{12} / \left(1 + \frac{1}{K_{23}^x} \left(1 + \frac{1}{K_{34I}^x} \right) \right) \quad \text{Eq. S40}$$

Using this equilibrium constant the fraction of T_3 -bound ribosomes is:

$$\frac{[R_{bound}]}{[R_{tot}]} = \frac{[T_3^x]}{[T_3^x] + K_{dl}^x} \quad \text{Eq. S41}$$

The same type of analysis applies to the binding of anticodon-stem-loop ASL constructs (6) to the ribosome. In cognate cases, K_{34I}^c and the product $K_{23}^c K_{34I}^c$ are small and ribosome-bound T_3 is predominantly in state C_4 with monitoring bases in contact with the codon-anticodon helix and the 30S subunit “closed” (6). Eq. S40 simplifies therefore to $K_{dl}^c \approx K_{12} K_{23}^c K_{34I}^c$, so that the 15-fold increase in ASL affinity caused by paromomycin (6) is accounted for by the 15-fold decrease in K_{34I}^c as estimated here from the increase in dissociation time of the GTPase-deficient ternary complexes. In near-cognate cases, K_{340}^{nc} in Eq. 40 is much larger than one (6) and remains larger than one even after paromomycin addition. Hence, the overall binding constant K_{dl}^{nc} decreases but slightly, as observed.

Reduction of a four-state to a three-state scheme for initial codon selection

In general, three (Eq. 17 in the main text) and four (Eq. S1 here) state schemes exhibit distinct kinetic patterns, but in special cases a three-state scheme with effective k_{e3I}^x and q_{e3I}^x parameters may behave as a four state scheme (Pavlov et al , 2017). One such case arises when there is comparatively rapid equilibration between C_3 and C_4 of the four-state scheme of Eq. S1. Under this condition the four-state scheme can be reduced to a three-state scheme with a combined state C_{34} and compounded rate constants k_{e3I}^x and q_{e3I}^x .



Indeed, assuming C_3 and C_4 equilibrated in the scheme in Eq. S1, one obtains:

$$\begin{aligned} q_{e3I}^x [C_{34}] &= q_{3I}^x [C_3] = q_{3I}^x [C_{34}] \frac{q_{4I}^x}{k_{3I} + q_{4I}^x} \\ k_{e3I}^x [C_{34}] &= k_{4I}^x [C_4] = k_{4I}^x [C_{34}] \frac{k_{3I}}{k_{3I} + q_{4I}^x} \end{aligned} \quad \text{Eq. S43}$$

Eq. S43 implies:

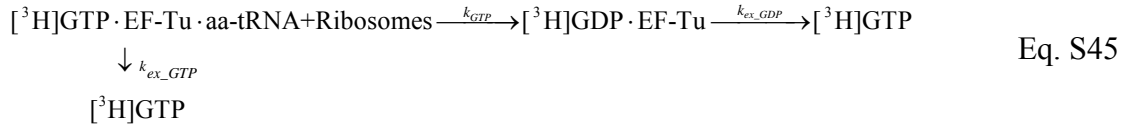
$$q_{e3I}^x = q_3^x \frac{K_{34I}^x}{1 + K_{34I}^x}$$

$$k_{e3I}^x = k_{4I}^x \frac{1}{1 + K_{34I}^x}$$

Eq. S44

Data analysis

Data were analyzed using Origin 7.5 (OriginLab Corp.). For cognate as well as fast near-cognate reactions, the rate of GTP hydrolysis (k_{GTP}) was estimated by fitting data to a single exponential model. For the slow, near-cognate measurements, where also the slow exchange of $[^3\text{H}]\text{GDP}$ and $[^3\text{H}]\text{GTP}$ on EF-Tu have to be considered, the following model was used:



The rate k_{GTP} for the near-cognate reaction was estimated by joint fitting the data for near-cognate and its corresponding cognate reaction, assuming that they have the same plateau (P) for GTP hydrolysis, the GDP dissociation rate from EF-Tu (k_{ex_GDP}), and the GTP exchange rate on ternary complex (k_{ex_GTP}). The following equation was used for the fitting:

$$\frac{[^3\text{H}]\text{GDP}}{[^3\text{H}]\text{GDP} + [^3\text{H}]\text{GTP}} = \frac{P \cdot k_{GTP}}{k_{ex_GDP} - (k_{GTP} + k_{ex_GTP})} \left(e^{-(k_{GTP} + k_{ex_GTP})t} - e^{-k_{ex_GDP}t} \right) + bg .$$

Eq. S46

Kinetic efficiencies, k_{cat}/K_m for both cognate and near-cognate reactions were calculated from the GTP hydrolysis rate as $(k_{cat} / K_m)^{c/nc} = k_{GTP}^{c/nc} / [R]$, where $[R]$ was the concentration of active ribosomes. Control experiment in which ribosome concentration was doubled resulted in doubling of k_{GTP} validating that the measurements were conducted in k_{cat}/K_m -range.

Supplementary discussion

Rodnina and coworkers used fast kinetics and T_3 s with fluorescently labeled tRNA to estimate the rate constants of the following scheme:



in the presence and absence of paromomycin (Par) (7). In this and previous studies (8,9) rate constant k_{-2} was directly estimated as the rate constant k_d of the single-exponential fluorescence decay observed in a chase experiment. In this experiment a pre-bound fluorescence labeled near-cognate ternary complex (T_{3f}) assembled with a non-hydrolysable GTP analogue was chased by addition of a large excess of non-fluorescent cognate T_3 (7). In this situation a dissociated fluorescence labeled near-cognate T_{3f} cannot rebind and the kinetic scheme for its dissociation is given by:



The inference (7-9) that $k_{-2} \approx k_d$ is invalid because the decay time $1/k_d$ depends not only on k_{-2} but also on k_2 , k_{-1} and fluorescence parameters of T_{3f} in states C_2 and C_3 . To see this we first consider two extreme scenarios. In the first $k_{-2} \gg k_2$ and the equilibrium before the chase is strongly shifted to C_2 . In this case, which pertains to non-cognate and some error-resilient near-cognate T_{3f} s, it is clear that $k_d \approx k_{-1}$ so that the chase experiments provide almost no information about k_{-2} . In the second scenario, which mainly pertains to cognate and error-prone near-cognate T_{3f} s, $k_{-2} \ll k_2$ and the equilibrium before the chase is strongly shifted to C_3 . In this case, T_{3f} originally in state C_3 , requires the average time $1/k_{-2}$ to transit to state C_2 from where it either dissociates with probability $p_d = k_{-1} / (k_2 + k_{-1})$ or returns to state C_3 with probability $k_2 / (k_2 + k_{-1})$. The number of trials before dissociation is given by $1/p_d = 1 + k_2 / k_{-1}$ with each trial taking time $1/k_{-2}$. The total

dissociation time is then the number of trials multiplied by the trial time: $1/k_d \approx (1+k_2/k_{-1})/k_{-2}$. It follows that $k_{-2} \approx (1+k_2/k_{-1}) \cdot k_d$ meaning that the approximation $k_{-2} \approx k_d$ underestimates k_{-2} by a factor $\approx (1+k_2/k_{-1})$, which, in cases $k_2 > k_{-1}$, may take values considerably larger than one.

A more general treatment of the kinetics of this chase experiment that takes into consideration also the fluorescence parameters involved is outlined below. It shows that, indeed, the approximation $k_{-2} \approx k_d$ underestimates k_{-2} by at least the factor k_2/k_{-1} that can be large under conditions of no initial selection (7-9). We note also that, since k_2 and k_3 in the scheme in Eq. S47 are obtained from a “global fit” with fixed input values of k_1 , k_{-1} and $k_{-2} \approx k_d$ (7-9), the estimates of k_2 and k_3 will also be affected by the underestimation of k_{-2} to an unknown extent.

Kinetics of the chase experiment in near-cognate cases

The fluorescence $F(t)$ in the chase experiment is given by:

$$F(t) = F_3 C_3(t) + F_2 C_2(t) + F_1 C_1(t) \quad \text{Eq. S49}$$

Here, F_3 , F_2 and F_1 refer to the fluorescence intensity per unit concentration of T_{3f} in states

C_3 , C_2 and free state C_1 , respectively. Introducing:

$$\begin{aligned} \Delta F_3 &= F_3 - F_1 \\ \Delta F_2 &= F_2 - F_1 \end{aligned} \quad \text{Eq. S50}$$

one obtains $F(t) - F_B = \Delta F_3 C_3(t) + \Delta F_2 C_2(t)$. Here $F_B = F_1 C_T(\infty)$ is the background fluorescence when all fluorescing T_{3f} has dissociated from the ribosome. The decay of fluorescence during the chase is conventionally described (7) by the reduction in “relative fluorescence” $f(t)$ defined as:

$$f(t) \equiv \frac{F(t) - F_B}{F_B} = \frac{\Delta F_3}{F_B} C_3(t) + \frac{\Delta F_2}{F_B} C_2(t) \quad \text{Eq. S51}$$

Introducing $f_3 = \Delta F_3 / F_B$ and $f_2 = \Delta F_2 / F_B$, $f(t)$ simplified to:

$$f(t) = f_3 C_3(t) + f_2 C_2(t) \quad \text{Eq. S52}$$

Time course $f(t)$ of fluorescence decay in the chase experiment can be easily obtained by solving the following equation system for the concentrations of complexes C_2 and C_3 in the scheme in Eq. S48:

$$\begin{aligned} \frac{dC_2(t)}{dt} &= -(k_2 + k_{-1})C_2(t) + k_{-2}C_3(t) \\ \frac{dC_3(t)}{dt} &= k_2C_2(t) - k_{-2}C_3(t) \end{aligned} \quad \text{Eq. S53}$$

The solution takes also into account the initial condition that right before the chase start the ribosome-bound T_{3f} has been equilibrated between states C_2 and C_3 . The solution shows that $f(t)$ is described by a two-exponential function as: $f(t) = A_1 e^{-\lambda_1 t} + A_2 e^{-\lambda_2 t}$ with the rate constants λ_1 and λ_2 given by the two eigenvalues of Eq. S53:

$$\begin{aligned} \lambda_1 &= \lambda_{slow} \approx k_{-2} \frac{k_{-1}}{k_2 + k_{-2} + k_{-1}} \\ \lambda_2 &= \lambda_{fast} \approx k_2 + k_{-2} + k_{-1} \end{aligned} \quad \text{Eq. S54}$$

Further, using a mean-time approach (1-3) it can be shown that the k_d -value obtained from a one-exponential fitting of $f(t)$ is well approximated by:

$$k_d \approx k_{-2} \frac{k_{-1}}{k_2 + k_{-2} + \alpha k_{-1}} \quad \text{Eq. S55}$$

where:

$$\alpha = \frac{k_2}{k_2 + (f_2 / f_3) k_{-2}} \quad \text{Eq. S56}$$

Parameter α depends on rate constants k_2 and k_{-2} and also on the ratio f_2 / f_3 of fluorescent parameters. We note also that $0 \leq \alpha \leq 1$ (see Eq. S56) and that the expression for k_d given by Eq. S55 coincides with the expression for the slow eigenvalue in Eq. S54 when $\alpha \approx 1$.

The value of k_{-2} is then estimated from Eq. S54 as:

$$k_{-2} \approx k_d \frac{k_2 + k_{-2} + \alpha k_{-1}}{k_{-1}} > k_d \frac{k_2 + k_{-2}}{k_{-1}} \quad \text{Eq. S57}$$

This shows that identification $k_{-2} \approx k_d$ underestimates k_{-2} by at least a factor of k_2 / k_{-1} .

Furthermore, with the estimated value $f_2 / f_3 \approx 0.3$ (9) and when $k_{-2} < k_2$ parameter $\alpha \approx 1$

and the underestimation becomes even more severe:

$$k_{-2} \approx k_d \frac{k_2 + k_{-2} + k_{-1}}{k_{-1}} \quad \text{Eq. S58}$$

References

1. Bilgin, N., Claesens, F., Pahverk, H. and Ehrenberg, M. (1992) Kinetic properties of Escherichia coli ribosomes with altered forms of S12. *J Mol Biol*, **224**, 1011-1027.
2. Borg, A., Pavlov, M. and Ehrenberg, M. (2016) Mechanism of fusidic acid inhibition of RRF- and EF-G-dependent splitting of the bacterial post-termination ribosome. *Nucleic Acids Res*, **44**, 3264-3275.
3. Borg, A., Holm, M., Shiroyama, I., Hauryliuk, V., Pavlov, M., Sanyal, S. and Ehrenberg, M. (2015) Fusidic acid targets elongation factor G in several stages of translocation on the bacterial ribosome. *J Biol Chem*, **290**, 3440-3454.
4. Fersht, A. (1977) *Enzyme structure and mechanism*. 1977 ed. W.H. Freeman and Company, New York.
5. Daviter, T., Wieden, H.J. and Rodnina, M.V. (2003) Essential role of histidine 84 in elongation factor Tu for the chemical step of GTP hydrolysis on the ribosome. *J Mol Biol*, **332**, 689-699.
6. Ogle, J.M., Murphy, F.V., Tarry, M.J. and Ramakrishnan, V. (2002) Selection of tRNA by the ribosome requires a transition from an open to a closed form. *Cell*, **111**, 721-732.
7. Pape, T., Wintermeyer, W. and Rodnina, M.V. (2000) Conformational switch in the decoding region of 16S rRNA during aminoacyl-tRNA selection on the ribosome. *Nat Struct Biol*, **7**, 104-107.
8. Pape, T., Wintermeyer, W. and Rodnina, M.V. (1998) Complete kinetic mechanism of elongation factor Tu-dependent binding of aminoacyl-tRNA to the A site of the E. coli ribosome. *Embo J*, **17**, 7490-7497.
9. Pape, T., Wintermeyer, W. and Rodnina, M. (1999) Induced fit in initial selection and proofreading of aminoacyl-tRNA on the ribosome. *Embo J*, **18**, 3800-3807.